

Study of the Gauge Mediation Signal with Non-pointing Photons at the CERN LHC

Kiyotomo Kawagoe,¹ Tomio Kobayashi,² Mihoko M. Nojiri,³ and Atsuhiko Ochi¹

¹*Department of Physics, Kobe University, Kobe 657-8501, Japan*

²*ICEPP, University of Tokyo, Tokyo 113-0033, Japan*

³*YITP, Kyoto University, Kyoto 606-8502, Japan*

(Dated: October 22, 2018)

Abstract

In this paper we study the gauge mediation signal with the ATLAS detector at the CERN LHC. We focus on the case where the NLSP is the long-lived lightest neutralino ($\tilde{\chi}_1^0$) which decays dominantly into a photon (γ) and a gravitino (\tilde{G}). A non-pointing photon from the neutralino decay can be detected with good position and time resolutions by the electromagnetometer (ECAL), while the photon momentum would be precisely measured if the photon is converted inside the inner tracking detector before reaching the ECAL. A new technique is developed to determine the masses of the slepton ($\tilde{\ell}$) and the neutralino from events with a lepton and a converted non-pointing photon arising from the cascade decay $\tilde{\ell} \rightarrow \ell \tilde{\chi}_1^0 \rightarrow \ell \gamma \tilde{G}$. A Monte Carlo simulation at a sample point shows that the masses would be measured with an error of 3% for $\mathcal{O}(100)$ selected $\ell\gamma$ pairs. Once the sparticle masses are determined by this method, the decay time and momentum of the neutralino are solved using the ECAL data and the lepton momentum only, for all $\ell\gamma$ pairs without the photon conversion. We estimate the sensitivity to the neutralino lifetime for $c\tau = 10$ cm to $\mathcal{O}(10)$ m.

PACS numbers: **12.60.Jv**, **14.80.Ly**

I. INTRODUCTION

Minimal Supersymmetric Standard Model (MSSM) is a promising candidate beyond the Standard Model. As the supersymmetry (SUSY) must be spontaneously broken, the MSSM needs an additional sector (the hidden sector) which breaks the supersymmetry while avoiding the FCNC problem. The origin of the SUSY breaking and the mediation to the MSSM sector are therefore the key feature of SUSY models. The hidden sector SUSY breaking are expressed in terms of the order parameter of the SUSY breaking F and the scale of the SUSY breaking mediation to the MSSM sector M . The mass scale of MSSM sparticles M_{SUSY} is then of the order of $\lambda F/M$, where λ is the coupling of the hidden sector to the MSSM sector. If $M \sim M_{pl}$, $M_{SUSY} = 1$ TeV corresponds to $\sqrt{F} \sim 10^{10}$ GeV. This class of mediation is called the supergravity (SUGRA) model. On the other hand, the SUSY breaking mediation may be due to renormalizable interactions, such as the gauge interaction. This is called “gauge mediation” (GM) models [1, 2]. In the GM models M and F are arbitrary and we expect $M \ll M_{pl}$.

The GM models are described by a few parameters. The MSSM gaugino masses M_i ($i = 1, 2, 3$) and slepton masses are of the order of $\alpha_i F/M$ in the simplest GM model, where α_i denotes each gauge coupling constant. On the other hand, the gravitino mass $m_{\tilde{G}}$ is proportional to F_0/M_{pl} where F_0 is the order of the SUSY breaking of the total system ($F_0 > F$) [3, 4].

Because $M \ll M_{pl}$, the lightest SUSY particle (LSP) is the gravitino (\tilde{G}) in the GM models. The next lightest SUSY particle (NLSP) is a particle in the MSSM sector which decays into a gravitino [5]. If the lightest neutralino ($\tilde{\chi}_1^0$) is the NLSP, the dominant decay mode is $\tilde{\chi}_1^0 \rightarrow \gamma \tilde{G}$. The neutralino lifetime $c\tau^1$ is a function of F_0 and $m_{\tilde{\chi}_1^0}$, and may be long-lived.

The CERN large hadron collider (LHC) is a pp collider at center of mass energy of 14 TeV. The LHC is expected to start its physics runs in 2007. The initial integrated luminosity will be $10 \text{ fb}^{-1}/\text{yr}$ at the beginning (low luminosity runs), and then upgrade to $100 \text{ fb}^{-1}/\text{yr}$ (high luminosity runs). Signatures of the GM models at the LHC are spectacular [6–8]. In the case of the neutralino NLSP, SUSY events have nearly always hard photons, which may

¹ In this paper the neutralino lifetime is multiplied by the light velocity c to have a dimension of length.

not be pointing to the interaction point (non-pointing photons).

In this paper we propose a new approach to study the signature of the GM models using the ATLAS detector at the LHC for the case where the neutralino NLSP dominantly decays into a photon and a gravitino with $c\tau$ longer than $\mathcal{O}(10)$ cm. We use two newly developed techniques. One is to determine the direction of the gravitino momentum by using the arrival position, arrival time, and momentum of the non-pointing photon, which are measured at the electromagnetic calorimeter (ECAL). The precision of the photon momentum would be significantly improved if the non-pointing photon is converted into an e^+e^- pair in the inner tracking detector located inside the ECAL. The other technique is the “mass relation method”, a mass reconstruction technique which does not rely on the conventional endpoint measurement [9]. In this method we use the fact that each event from a same cascade decay satisfies mass shell conditions of intermediate particles. These techniques are described in Sec. II and a simulation is carried out in Sec. III. A fast Monte Carlo simulation shows that, using the new techniques, *statistical error* of the masses of $\tilde{\ell}$ and $\tilde{\chi}_1^0$ can be a few % for $\mathcal{O}(100)$ selected $\ell\gamma$ pairs from the decay chain $\tilde{\ell} \rightarrow \ell\tilde{\chi}_1^0 \rightarrow \ell\gamma\tilde{G}$. Although more works, especially full detector simulations, are needed to establish the techniques, the result of the fast simulation is quite encouraging.

In Sec. IV we show that events with $\ell\gamma$ pairs are fully reconstructed by using the measured mass and the ECAL information. This measurement is utilized to determine the neutralino lifetime for $10 \text{ cm} < c\tau < \mathcal{O}(10) \text{ m}$. This analysis does not require the photon to be converted in the inner detector. Therefore available number of events is significantly larger. Finally in Sec. V we discuss how these measurements would be translated into the fundamental parameters F_0 , F and M in the GM models.

II. KINEMATICS OF THE EVENTS WITH NON-PROMPT $\tilde{\chi}_1^0$ DECAY

We first discuss the decay kinematics of the neutralino with an unnegligible lifetime. In FIG. 1 we schematically show a neutralino decaying into a gravitino and a photon in the ATLAS detector. The neutralino is produced at the interaction point O at the time $t = 0$, and then flies to the decay point D, where the neutralino decays at $t = t_D$ into a photon and a gravitino. The photon goes to the point A in the ECAL at $t = t_\gamma$. We define two angles α and ψ , the former between the photon momentum \vec{p}_γ and the position vector $\vec{x}_\gamma = \overrightarrow{OA}$,

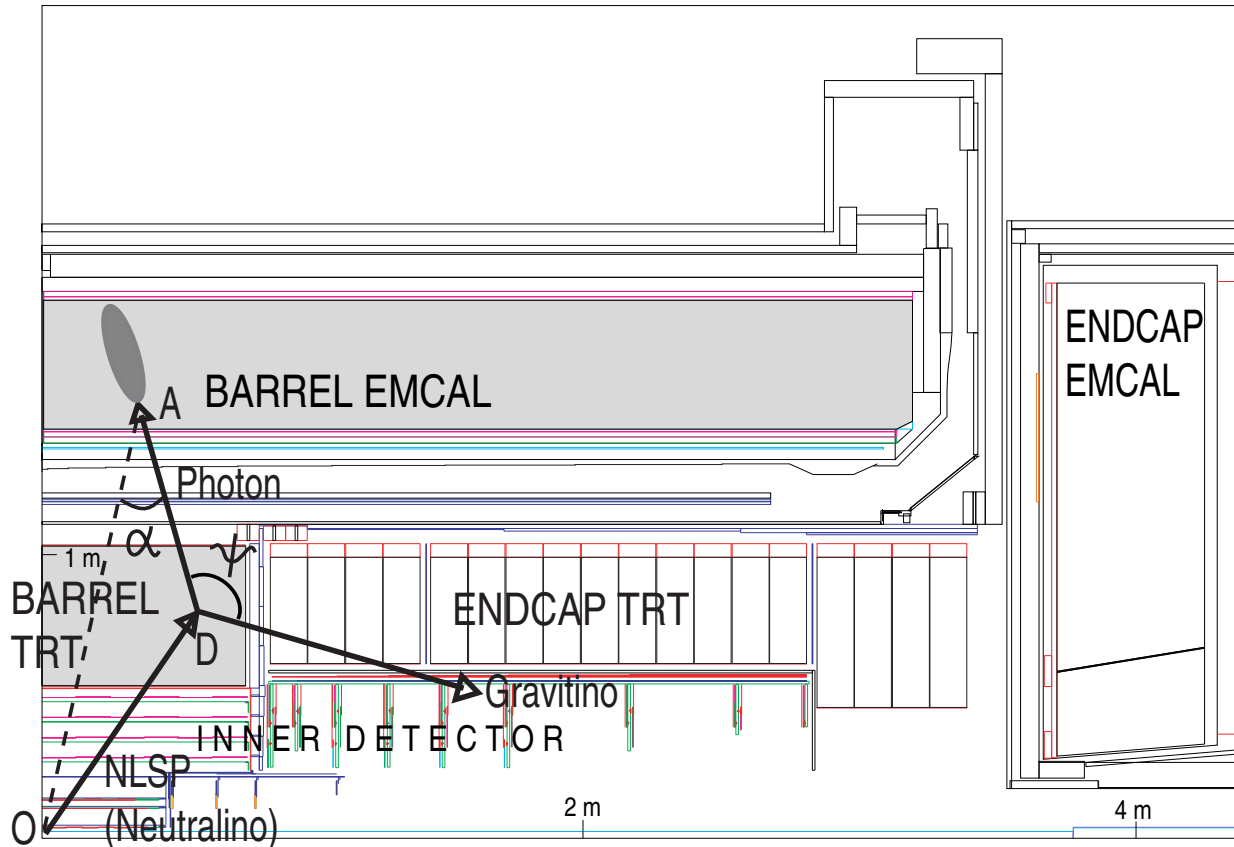


FIG. 1: Decay kinematics of the NLSP (the lightest neutralino $\tilde{\chi}_1^0$) in the ATLAS detector.

and the latter between \vec{p}_γ and the gravitino momentum $\vec{p}_{\tilde{G}}$.

We can experimentally measure α , t_γ and the distance $L = |\vec{OA}|$. The angle ψ can then be calculated from the three observable as

$$\cos \psi = \frac{1 - \xi^2}{1 + \xi^2},$$

$$\text{where } \xi \equiv \frac{ct_\gamma - L \cos \alpha}{L \sin \alpha}. \quad (1)$$

Because the three momenta $\vec{p}_{\tilde{\chi}}$, \vec{p}_γ and $\vec{p}_{\tilde{G}}$ are on a same plane, the direction of the gravitino momentum is completely determined².

The information of the gravitino direction may be used to determine the sparticle masses. We describe this idea for the decay chain $\tilde{\ell} \rightarrow \ell \tilde{\chi}_1^0 \rightarrow \ell \gamma \tilde{G}$. The slepton $\tilde{\ell}$ may be copiously

² The formula can be shown quite easily by going into the frame where the interaction point and the detection point is same. We define the rapidity of the gravitino and photon, taking the boost direction as the z direction. To obtain the formula Eq. (1) one then goes back to the laboratory frame noting the additivity of the rapidity. We thank Dr. Odagiri for pointing out this.

produced at the LHC from $\tilde{\chi}_2^0$ or $\tilde{\chi}_1^\pm$ decays, where $\tilde{\chi}_2^0$ and $\tilde{\chi}_1^\pm$ are dominantly produced from gluino or squark decays. The neutralino and slepton masses ($m_{\tilde{\chi}_1^0}$ and $m_{\tilde{\ell}}$) are related by the following formula;

$$\begin{aligned}
m_{\tilde{\ell}}^2 &= (p_\gamma + p_{\tilde{G}} + p_\ell)^2 \\
&= 2E_\gamma E_{\tilde{G}}(1 - \cos \psi) + 2E_\ell E_{\tilde{G}}(1 - \cos \theta_{\ell\tilde{G}}) \\
&\quad + 2E_\ell E_\gamma(1 - \cos \theta_{\ell\gamma}) \\
&= \left(1 + \frac{E_\ell(1 - \cos \theta_{\ell\tilde{G}})}{E_\gamma(1 - \cos \psi)}\right) m_{\tilde{\chi}_1^0}^2 + 2E_\ell E_\gamma(1 - \cos \theta_{\ell\gamma}) \\
&\equiv am_{\tilde{\chi}_1^0}^2 + b,
\end{aligned} \tag{2}$$

where we use the relation

$$\begin{aligned}
m_{\tilde{\chi}_1^0}^2 &= (p_\gamma + p_{\tilde{G}})^2 \\
&= 2E_\gamma E_{\tilde{G}}(1 - \cos \psi),
\end{aligned} \tag{3}$$

and neglect the lepton and gravitino masses. A pair of parameters (a, b) can be calculated event by event from the momenta of the lepton and the photon, and the direction of the gravitino momentum. Because the sparticle masses $m_{\tilde{\chi}_1^0}$ and $m_{\tilde{\ell}}$ should be common for all events, one can determine them if we have at least two tagged events.

In Refs. [9, 10] the masses $m_{\tilde{\chi}_1^0}$ and $m_{\tilde{\ell}}$ are determined by measuring endpoints of mass distributions for events containing $\ell\ell\gamma$ which come from the decay chain $\tilde{\chi}_2^0 \rightarrow \ell\tilde{\ell} \rightarrow \ell\ell\tilde{\chi}_1^0 \rightarrow \ell\ell\gamma\tilde{G}$. Endpoints in the distributions of invariant masses $m_{\ell\ell}$, $m_{\ell\gamma}$, and $m_{\ell\ell\gamma}$ are combined to solve $m_{\tilde{\ell}}$, $m_{\tilde{\chi}_1^0}$ and $m_{\tilde{\chi}_2^0}$. Note that only the events near the endpoints contribute to the mass determination in the endpoint analysis.

Our proposal is quite different from the endpoint analysis. We assume a set of events come from a common cascade decay, and use the mass shell condition of the sparticles involved in the cascade decay. Each event gives an independent constraint to the masses as given in Eq. (2), and contributes to the mass determination. We call this “the mass relation method”. This technique may be applied for other cascade decays of SUSY particles, which will be discussed in future publications.

The ATLAS detector at the LHC has a good capability to measure non-pointing photons, where the barrel part of the electromagnetic calorimeter (ECAL) and the transition radiation tracker (TRT) will play important roles (FIG. 1). The barrel ECAL is a liquid-Argon

calorimeter, and covers the psuedo-rapidity range $|\eta| < 1.4$. The inner radius of the ECAL is 150 cm. We assume the angular resolutions of the photon arrival point at the ECAL inner surface to be $\sigma_\phi \sim 0.004$ and $\sigma_\eta \sim 0.002$. The ECAL energy resolution is expected to be $\sigma_{E_\gamma}/E_\gamma = 10\%/\sqrt{E_\gamma}$, where the photon energy E_γ is given in GeV. The longitudinal and transverse segmentation of the ECAL gives a measure of the development of electromagnetic showers. The first longitudinal sampling is finely segmented in the η direction, resulting in a good angular resolution of $\sigma_\theta = 60 \text{ mrad}/\sqrt{E_\gamma}$, where θ is the polar angle of the photon momentum with respect to the beam axis. The azimuthal angle ϕ of the photon momentum is only poorly measured by the ECAL, as the segmentation is very coarse in this direction. The ECAL also has an excellent time resolution, $\sigma_{t_\gamma} < 100 \text{ ps}$ for $E_\gamma > 30 \text{ GeV}$, confirmed by a test-beam experiment.

When a photon is pointing to the interaction point, the photon momentum is precisely determined by the ECAL only, namely by measuring the energy deposit and the arrival position. However, in the case of the GM models, the photon is in general non-pointing, and the transverse components of the photon momentum are only poorly measured. Fortunately, the barrel TRT is located inside the barrel ECAL as a component of the inner tracking detector. This detector covers the radial range from 56 to 107 cm and the pseudo-rapidity range $|\eta| < 0.7$. As the straw tube trackers of the barrel TRT are parallel to the beam axis, trajectories of charged particles are precisely measured in the r - ϕ plane. If a photon is converted into an e^+e^- pair before escaping the barrel TRT, the ϕ angle of the photon momentum can be very precisely measured. As the ϕ angle resolution is much better than the θ angle resolution by the ECAL, the resolution of the angle α becomes $\sigma_\alpha = \sqrt{\sigma_\theta^2 + \sigma_\phi^2} \sim \sigma_\theta$. The material thickness of the TRT is about 10% of one radiation length at $\eta \sim 0$. Namely $\sim 10\%$ of photons will be converted in the TRT.

III. RECONSTRUCTION OF GRAVITINO DIRECTION AND SPARTICLE MASSES

In order to test the new techniques we perform a Monte Carlo event simulation at GM point G1 [9, 10] with F_0 , or equivalently the neutralino lifetime $c\tau$, being the only free parameter. The model parameters and some of sparticle masses are listed in TABLE I. The low energy SUSY parameters are calculated by ISASUSY 7.51, and the mass spectrum, the

TABLE I: Model parameters and some of the sparticle masses at point G1. The parameter N is an integer number which appears in Eq. (10).

Parameters	Sparticle masses (GeV)		
$F/M = 90$ TeV	$m_{\tilde{g}} = 720$	$m_{\tilde{\ell}_L} = 324$	$m_{\tilde{\chi}_1^0} = 117$
$M = 500$ TeV	$m_{\tilde{q}_L} = 958$	$m_{\tilde{\ell}_R} = 162$	$m_{\tilde{\chi}_2^0} = 217$
$N = 1$	$m_{\tilde{q}_R} = 915$	$m_{\tilde{t}_1} = 831$	$m_{\tilde{\chi}_3^0} = 420$
$\tan \beta = 5$		$m_{\tilde{b}_1} = 909$	$m_{\tilde{\chi}_4^0} = 442$
$\mu > 0$			

couplings and the decay branching ratios are interfaced to HERWIG version 6.4. We generate 10^5 SUSY events at this point, corresponding to an integrated luminosity of 13.9 fb^{-1} . When we simulate the events, we keep the lightest neutralinos (NLSPs) stable at the generator level. Then a fast detector simulator ATLFast is used for all particles except the neutralinos. The decay of the neutralinos and the photon conversions are simulated at the analysis stage. The photon conversion probability is estimated based on the detector thickness of the TRT [9]. If (a) a neutralino decays into a photon and a gravitino before escaping the TRT region, (b) the photon points to the barrel ECAL, and (c) the photon is converted inside the barrel TRT, then the energy, position, time, and direction of the photon are smeared by the Gaussian distribution according to their resolutions. The detector resolutions assumed in the simulation are listed in TABLE II. We assume the time resolution of the ECAL to be constant $\sigma_{t_\gamma} = 100$ ps for $E_\gamma > 30$ GeV.

For a moment we set the neutralino lifetime to be $c\tau = 100$ cm. In this case the neutralinos efficiently decay in the TRT, as the outer radius of the TRT is roughly 100 cm. We first apply pre-selection cuts to suppress the Standard Model background:

$$\begin{aligned}
 & \text{i) } M_{\text{eff}} > 400 \text{ GeV,} \\
 & \text{ii) } E_{\text{T}}^{\text{miss}} > 0.1 M_{\text{eff}}.
 \end{aligned} \tag{4}$$

The missing transverse energy $E_{\text{T}}^{\text{miss}}$ is calculated from the reconstructed jets, leptons, photons and unreconstructed calorimeter energies. The effective mass is defined by the sum of the missing transverse energy and the transverse momenta of the four hardest jets:

$$M_{\text{eff}} = E_{\text{T}}^{\text{miss}} + p_{\text{T},1} + p_{\text{T},2} + p_{\text{T},3} + p_{\text{T},4} \tag{5}$$

TABLE II: Detector resolutions assumed in our Monte Carlo simulation of non-pointing photons. The photon energy E_γ is given in GeV. As for the ϕ angle of the photon momentum, we assume the photon conversion in the TRT detector.

Observable		Detector	Resolution
Photon energy	E_γ	ECAL	$0.1\sqrt{E_\gamma}$
Photon arrival time	t_γ	ECAL	100 ps
Photon arrival position	η	ECAL	0.002
	ϕ	ECAL	0.004
Photon momentum	θ	ECAL	$0.060/\sqrt{E_\gamma}$
	ϕ	TRT	0.001

We do not include photons from the neutralino decays in the above calculation. The efficiency of the pre-selection cuts for the generated SUSY events is 80%.

The following cuts³ are then applied to select good ‘non-pointing’ photons with conversion in the TRT:

- 1) $E_\gamma > 30$ GeV,
- 2) $\alpha > 0.2$,
- 3) $\Delta t_\gamma (\equiv t_\gamma - L/c) > 1.0$ ns. (6)

The distributions of E_γ , α and Δt_γ are shown in FIGs. 2(a)–(c), where the cuts 1)–3) are sequentially applied.

In FIG. 2(d) we plot $\Delta\psi \equiv \psi - \psi_{\text{true}}$, where ψ is calculated from the measured L , α , and t_γ using Eq. (1) and ψ_{true} is the true value obtained from the generator information. The resolution σ_ψ is better than 40 mrad in this case.

In order to determine the masses of the slepton and the neutralino which appear in the cascade decay $\tilde{\ell} \rightarrow \ell \tilde{\chi}_1^0 \rightarrow \ell \gamma \tilde{G}$, isolated leptons (electrons and muons) with transverse momentum larger than 20 GeV are searched for to make a pair with the non-pointing photon. If there are several leptons in an event, we choose the $\ell\gamma$ pair which minimizes the invariant mass $m_{\ell\gamma}$. The parameters a and b are calculated for each $\ell\gamma$ pair. The scatter plot in the

³ Isolation from tracks/clusters is yet to be examined.

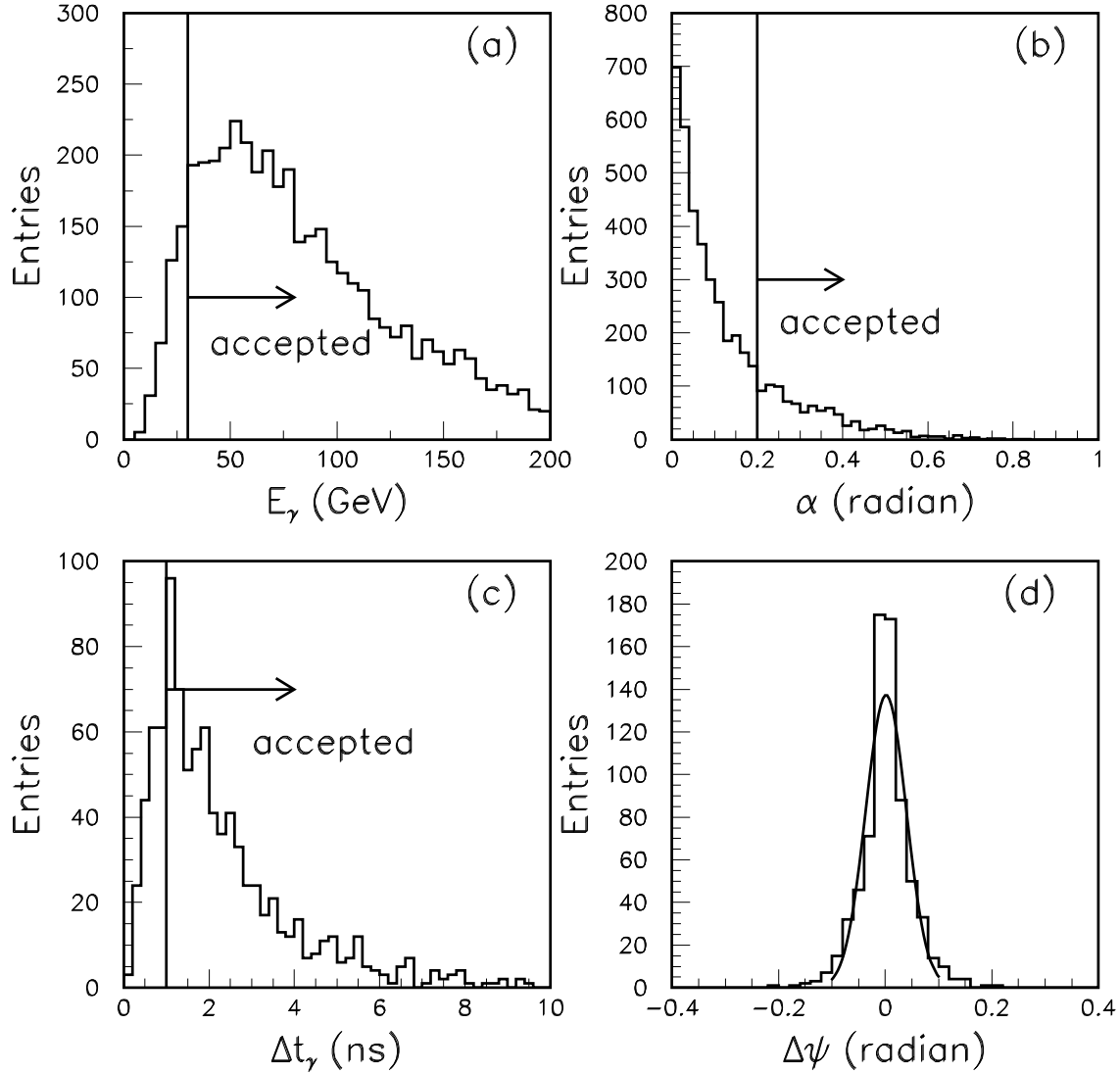


FIG. 2: Distributions of (a) E_γ , (b) α , and (c) Δt_γ at point G1 with $c\tau = 100$ cm, where the cuts 1)–3) in Eq. (6) are sequentially applied. (d) Distribution of $\Delta\psi \equiv \psi - \psi_{\text{true}}$ after applying the cuts, where ψ is the angle between the momenta of the photon and the gravitino. The result of a Gaussian fit is also shown.

(a, b) plane is shown in FIG. 3(a), where the sample contains about 120 $\ell\gamma$ pairs. The points are clearly concentrated along a line. The section of the b axis and the slope of the line must correspond to m_ℓ^2 and $m_{\tilde{\chi}_1^0}^2$ because of the relation $b = m_\ell^2 - m_{\tilde{\chi}_1^0}^2 a$. In FIG. 3(b) we take a simple average of (a, b) for the events between the two dotted lines in FIG. 3(a) by dividing

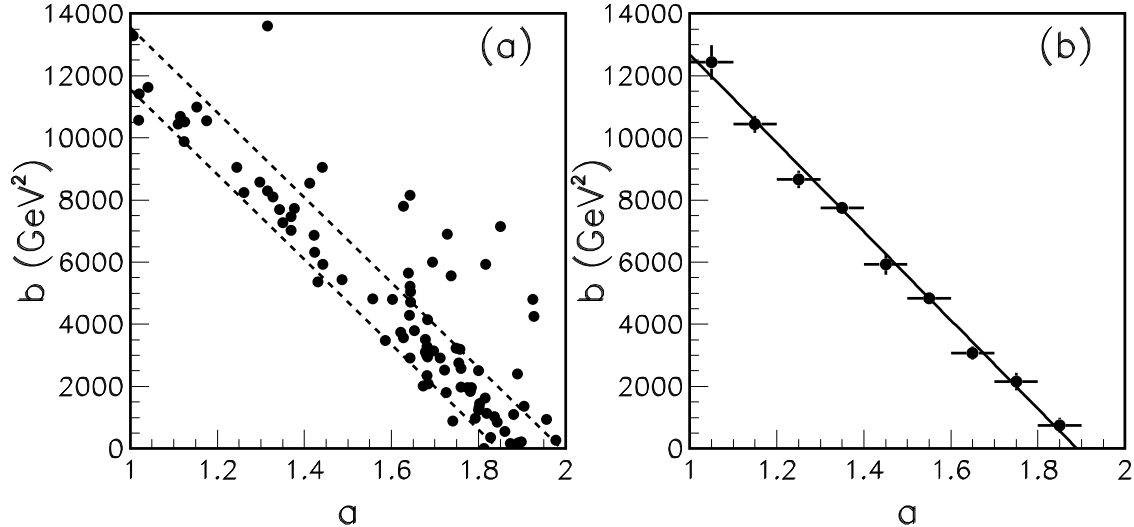


FIG. 3: (a) Distribution of $\ell\gamma$ pairs in (a, b) plane. The region between dotted lines shows our selection cut. (b) Points show the average values of (a, b) between the two dotted lines in (a). The region is divided into 9 bins. The solid line shows a result of a linear fit.

the region of a into 9 bins, and we fit the averaged data by the linear function Eq. (2). The fit results are $m_{\tilde{\ell}} = 162.1$ GeV and $m_{\tilde{\chi}_1^0} = 117.5$ GeV, while the input values are 161.7 GeV and 117.0 GeV, respectively.

To estimate errors of the mass measurement, the simulation and the fit are repeated 100 times with different random number seeds. The fitted masses are plotted in FIG. 4. By fitting the distribution, we obtain the errors of the masses as $\sigma_{m_{\tilde{\ell}}} = 2.7$ GeV and $\sigma_{m_{\tilde{\chi}_1^0}} = 3.5$ GeV. They correspond to relative mass errors of $2 \sim 3\%$. If one of the sparticle masses is precisely determined by some other measurements, the other sparticle mass can be determined with a precision of ~ 300 MeV by the mass relation method.

IV. FULL RECONSTRUCTION AND LIFETIME MEASUREMENT

In this section we demonstrate full reconstruction of the cascade decay $\tilde{\ell} \rightarrow \ell\tilde{\chi}_1^0 \rightarrow \ell\gamma\tilde{G}$, and we show that the neutralino lifetime can be determined by the reconstructed decay time and momentum of the neutralino. This analysis becomes possible after the precise

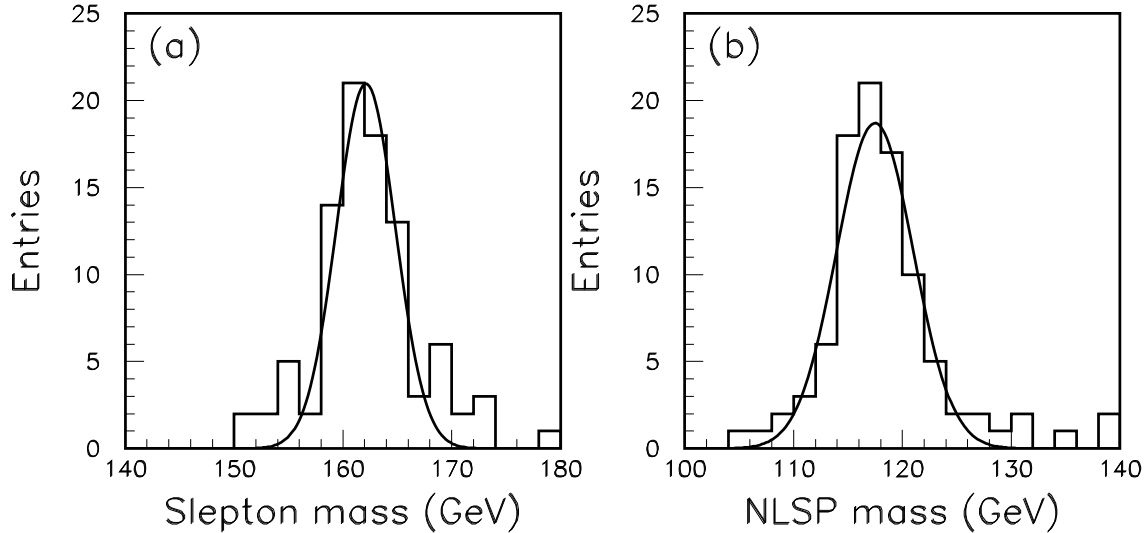


FIG. 4: Distributions of the fit results of (a) the slepton mass $m_{\tilde{\ell}}$ and (b) the neutralino mass $m_{\tilde{\chi}_1^0}$. The simulation and the fit are repeated 100 times with different random number seeds. Results of Gaussian fitting are also shown.

determination of $m_{\tilde{\ell}}$ and $m_{\tilde{\chi}_1^0}$ described in the previous section.

Here we study events with leptons and non-pointing photons, where the photons may or may not be converted in the inner detector. For each $\ell\gamma$ pair, the arrival time t_γ , arrival point \vec{x}_γ and energy E_γ of the photon, the longitudinal component of the photon momentum, and the lepton momentum \vec{p}_ℓ would be directly measured, while the transverse components of the photon momentum, the neutralino four momentum $p_{\tilde{\chi}}$ and its decay time t_D ($< t_\gamma$) are not directly measured. On the other hand, we have the following equations involving the unknown quantities,

$$\begin{aligned}
 \vec{v}_{\tilde{\chi}} t_D + \vec{v}_\gamma (t_\gamma - t_D) &= \vec{x}_\gamma, \\
 (p_{\tilde{\chi}} + p_l)^2 &= m_{\tilde{\ell}}^2, \\
 (p_{\tilde{\chi}} - p_\gamma)^2 &= p_G^2 = m_G^2 = 0, \\
 p_{\tilde{\chi}}^2 &= m_{\tilde{\chi}}^2,
 \end{aligned} \tag{7}$$

where $\vec{v}_{\tilde{\chi}}$ and \vec{v}_γ are velocity vectors ($|\vec{v}_\gamma| = c$), and the lepton and gravitino masses are neglected. Provided that we know the two masses $m_{\tilde{\ell}}$ and $m_{\tilde{\chi}_1^0}$, we can solve all the unknown

parameters from the equations. There are two solutions for each $\ell\gamma$ pair, which we obtain by numerically solving Eq. (7).

The simulation and analysis are modified from those of the previous section. The neutralino must decay inside the ECAL and the photon from the neutralino decay must enter the barrel ECAL, resulting in a much larger fiducial decay volume. We assume the fiducial volume as $r < 150$ cm and $|z| < 300$ cm, where r and z are the radial distance from the beam axis and the distance from the interaction point along the beam axis, respectively. In addition, as the photon conversion is not required in the inner detector, the acceptance of the events further increases. After applying the pre-selection cuts given in Eq. (4), we select non-pointing photons by the following cuts;

$$\begin{aligned}
 &1) \quad E_\gamma > 30 \text{ GeV}, \\
 &2) \quad \Delta\theta > 0.2 \text{ rad}, \\
 &3) \quad \Delta t_\gamma > 1 \text{ ns}.
 \end{aligned}
 \tag{8}$$

Here $\Delta\theta \equiv \theta_{\vec{p}_\gamma} - \theta_{\vec{x}_\gamma}$ is the difference between the polar angles of \vec{p}_γ and \vec{x}_γ , where the polar angles are measured from the beam axis. Note that the cut 2) is different from that in Eq. (6), because one cannot determine the angle α without precise measurement of the ϕ angle using the photon conversion. This $\Delta\theta$ cut is less efficient than the α cut in Eq. (6). However, the overall selection efficiency of this analysis is much larger because we have the larger fiducial decay volume and do not require the photon conversion in the inner detector.

Isolated leptons with transverse momentum larger than 20 GeV are used to make $\ell\gamma$ pairs. For each $\ell\gamma$ pair, there are two solutions for decay kinematics. We take solutions if the reconstructed decay points are in the fiducial volume (e.g. $r < 100$ cm and $|z| < 300$ cm). Therefore each $\ell\gamma$ pair may be counted twice. If there are several leptons in an event, all leptons are tried for each non-pointing photon, and accepted if the $\ell\gamma$ pair satisfies the fiducial condition.

In FIG. 5(a) we show a scatter plot of the reconstructed decay time t_D and the true decay time for $c\tau = 100$ cm. Here we use the input $m_{\tilde{\ell}}$ and $m_{\tilde{\chi}_1^0}$ for reconstruction. This plot shows that the neutralino decay time is correctly reconstructed for a significant fraction of the events. We also show the distribution of t_D/γ_χ in FIG. 5(b) for $c\tau = 50$ cm, 100 cm, and 200 cm, where the factor $1/\gamma_\chi$ corrects the effect of Lorentz boost. The distribution shows the expected exponential damping toward large t_D/γ_χ values. The geometric acceptance of

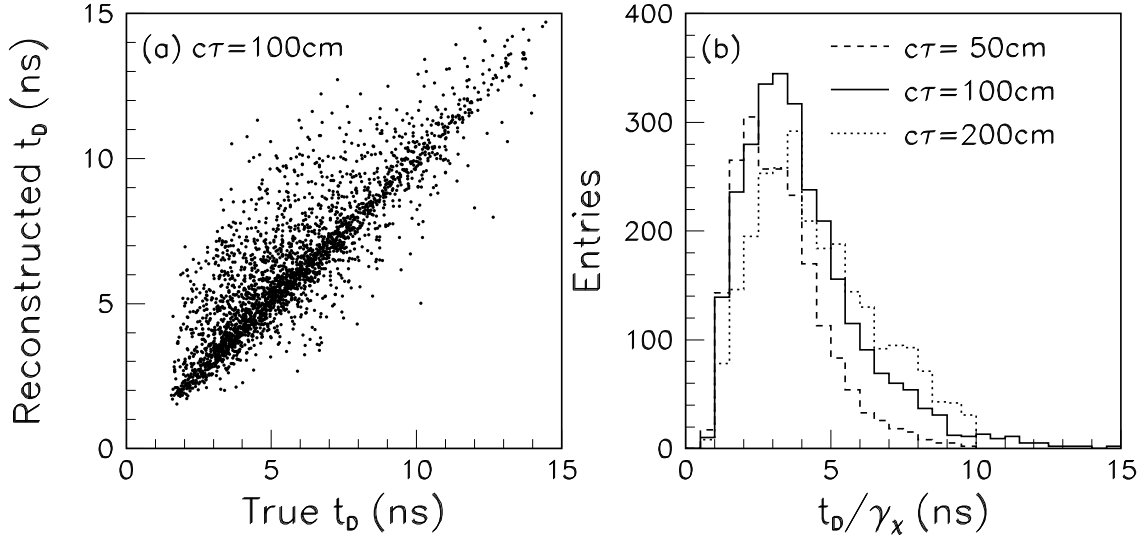


FIG. 5: (a) The distribution of the neutralino decay time t_D vs the true value. (b) Distributions of t_D/γ_χ for $c\tau = 50$ cm (dashed), 100 cm (solid) and 200 cm (dotted).

the events would be small when $c\tau\gamma_\chi > R_{in}$ or $\tau\gamma_\chi < 1$ ns, where R_{in} (~ 150 cm) is the inner radius of the ECAL and 1 ns is our cut value on the difference of the photon arrival time.

The geometric effect to the acceptance may be corrected by a study with full detector simulations. The momentum distribution of the neutralino would be an important uncertainty, as the transverse momentum distribution should depend on the gluino and squark masses. The heavier sparticle masses may be measured precisely by the $j\tilde{\chi}_1^0$ or $jj\tilde{\chi}_1^0$ invariant mass distribution for selected jets (j) and a neutralino, where the neutralino momentum is reconstructed by solving Eqs. (7). Therefore, we assume the systematics due to the momentum distribution of the neutralino would be small enough.

Assuming that the systematic errors are controlled, we may study the sensitivity to the lifetime $c\tau$ using the two measured values;

- (a) $\langle t_D/\gamma_\chi \rangle$: the average of the corrected decay time,
- (b) $N_{\ell\gamma}$: the number of accepted $\ell\gamma$ pairs. Note that we do not count an $\ell\gamma$ pair more than once to avoid over-counting.

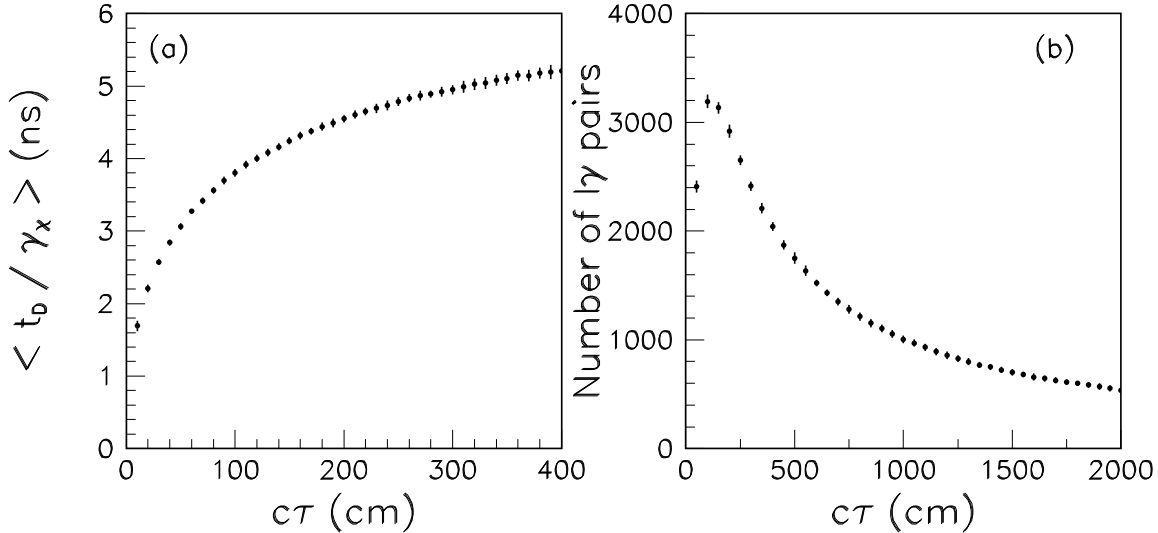


FIG. 6: (a) Average $\langle t_D / \gamma_\chi \rangle$ and (b) $N_{\ell\gamma}$ as functions of $c\tau$ for an integrated luminosity of 13.9 fb^{-1} at point G1. A dot and an error bar show the mean value and the standard deviation of 100 simulations at each $c\tau$ value, respectively.

They are plotted as functions of $c\tau$ in FIG. 6, where we repeat the simulation for an integrated luminosity of 13.9 fb^{-1} hundred times to obtain the mean $\langle t_D / \gamma_\chi \rangle$ and $N_{\ell\gamma}$ values and their standard deviations. In the plot, $\langle t_D / \gamma_\chi \rangle$ is larger than 1 ns even for $c\tau = 10$ cm because of the cut $\Delta t_\gamma > 1$ ns. Note that we do not have sensitivity on ψ when $c\tau < 10$ cm because the time resolution is ~ 0.1 ns, and $c \times 0.1 \text{ ns} \sim 3$ cm. The number of $\ell\gamma$ pairs with photon conversion ($N_{\ell\gamma}^{\text{conv}}$) is 13.0 and 80.5 for $c\tau = 10$ cm and $c\tau = 30$ cm, respectively. As the number of converted photons is rather small for $c\tau = 10$ cm, a large integrated luminosity is needed to determine the sparticle masses. For large $c\tau$ values, the average $\langle t_D / \gamma_\chi \rangle$ is saturated since most of the neutralinos decay outside the detector. Indeed the number of the reconstructed events takes its maximum at $c\tau \sim 100$ cm and decreases monotonically as shown in FIG. 6(b).

The sensitivity of the $\langle t_D / \gamma_\chi \rangle$ measurement to the lifetime $c\tau$ is estimated by the error of the measurement $\Delta \langle t_D / \gamma_\chi \rangle$. Namely we define the error of the lifetime $\Delta c\tau$ by the following formula:

$$g(c\tau \pm \Delta c\tau) = \langle t_D / \gamma_\chi \rangle \pm \Delta \langle t_D / \gamma_\chi \rangle, \quad (9)$$

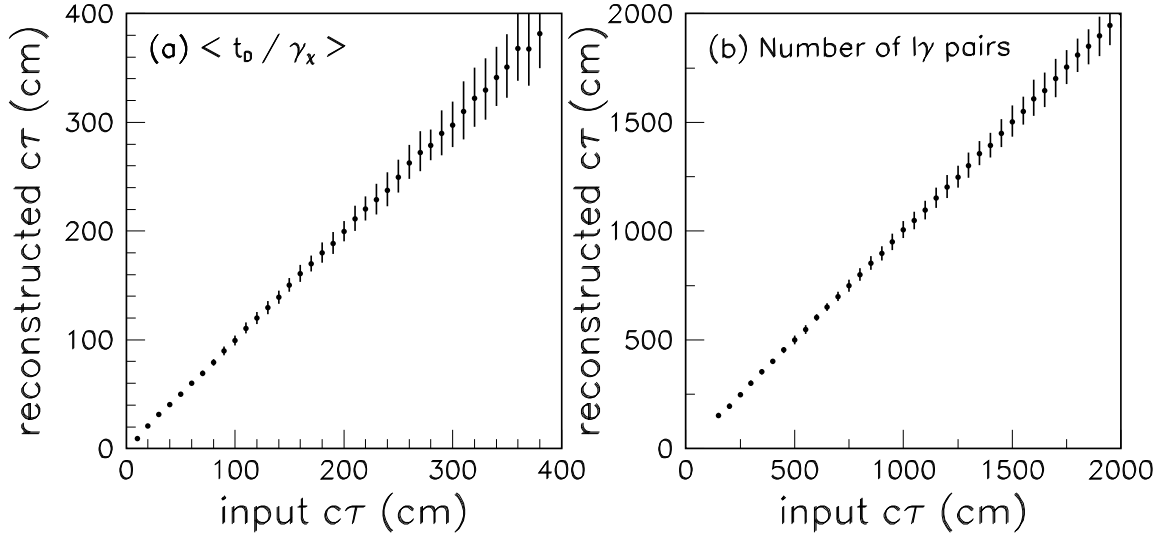


FIG. 7: Estimated resolution of the lifetime $c\tau$ for an integrated luminosity of 13.9 fb^{-1} from (a) the average $\langle t_D / \gamma_\chi \rangle$ and (b) the number of $\ell\gamma$ pairs $N_{\ell\gamma}$. The input $m_{\tilde{\ell}}$ and $m_{\tilde{\chi}_1^0}$ are used for the reconstruction and their errors are ignored.

where $g(c\tau)$ is a function to describe the average $\langle t_D / \gamma_\chi \rangle$. This function is numerically obtained by fitting the $\langle t_D / \gamma_\chi \rangle$ to a second power polynomial function of $c\tau$ using the average values in the region within $c\tau \pm 50$ cm. When $c\tau \gg 100$ cm, most of the neutralinos decay after reaching the ECAL and $\langle t_D / \gamma_\chi \rangle$ loses the sensitivity to $c\tau$. On the other hand, the number of the $\ell\gamma$ pairs $N_{\ell\gamma}$ sensitively reduces when $c\tau$ is longer than 100 cm. We can estimate the sensitivity of $N_{\ell\gamma}$ to $c\tau$ in a same way. The result is shown in FIG .7 and summarized in TABLE III. Note that we ignore the errors of $m_{\tilde{\ell}}$ and $m_{\tilde{\chi}_1^0}$ for a moment and use the input mass values. Note also that only statistical errors are considered here. Systematic errors are yet to be studied with full detector simulations.

For large $c\tau$ values the number of selected events is limited. In TABLE IV we summarize $N_{\ell\gamma}$ and $N_{\ell\gamma}^{\text{conv}}$ for an integrated luminosity of 13.9 fb^{-1} . For $c\tau < 2000$ cm the number $N_{\ell\gamma}^{\text{conv}}$ still exceeds 130 events if we assume an integrated luminosity of 100 fb^{-1} at point G1. Therefore, it might be still possible to determine the neutralino and slepton masses.

TABLE III: Relative resolution of $c\tau$. As in FIG. 7 (a) and (b) are estimated from the average $\langle t_D/\gamma_X \rangle$ and the number of $\ell\gamma$ pairs $N_{\ell\gamma}$, respectively.

(a) From $\langle t_D/\gamma_X \rangle$		(b) From $N_{\ell\gamma}$	
$c\tau$ (cm)	$\Delta c\tau/c\tau$	$c\tau$ (cm)	$\Delta c\tau/c\tau$
10	0.173	200	0.062
20	0.062	250	0.038
30	0.041	300	0.034
40	0.036	350	0.036
50	0.037	400	0.030
60	0.027	450	0.031
70	0.037	500	0.040
80	0.039	600	0.025
90	0.043	700	0.037
100	0.045	800	0.037
150	0.043	900	0.037
200	0.047	1000	0.039
250	0.061	1500	0.048
300	0.070	2000	0.033

TABLE IV: Number of $\ell\gamma$ pairs for an integrated luminosity of 13.9 fb^{-1} . $N_{\ell\gamma}^{\text{conv}}$ is the number of $\ell\gamma$ pairs with photon is conversion in the inner detector.

$c\tau$ (cm)	$N_{\ell\gamma}$	$N_{\ell\gamma}^{\text{conv}}$
10	147	13.0
30	1424	80.5
100	3193	116.3
300	2413	72.8
2000	536	14.3

V. DETERMINATION OF THE FUNDAMENTAL PARAMETERS

In this section we utilize the measurement of the sparticle masses and the neutralino lifetime to determine more fundamental parameters in the GM scenario. From the measurement of the slepton and neutralino masses, the ratio F/M is determined with a precision of a few %. This can be seen in the expression of the masses at the messenger scale as [11];

$$\begin{aligned} M_i &= \frac{\alpha_i(M)}{4\pi} \frac{F}{M} N \times g(F/M^2) \\ m_{\tilde{\ell}_R}^2 &= \frac{3\alpha_1^2(M)}{40\pi^2} \frac{F^2}{M^2} N \times f(F/M^2) \\ m_{\tilde{\ell}_L}^2 &= \left(\frac{3\alpha_1^2(M)}{160\pi^2} + \frac{3\alpha_2^2(M)}{32\pi^2} \right) \frac{F^2}{M^2} N \times f(F/M^2) , \end{aligned} \quad (10)$$

where N is an integer number, while g and f are some functions which satisfy $f(0) = g(0) \sim 1$ for $F \ll M^2$. The sparticle masses are proportional to F/M in this limit.

The absolute size of M (or F) is rather difficult to determine because it only appears through the sfermion mass running from M to the SUSY scale. A study [9] shows that the relative error $\Delta M/M$ is $\sim 30\%$ with 1% mass errors at this point.

The neutralino lifetime depends on the order parameter of the total SUSY breaking F_0 and the neutralino mass $m_{\tilde{\chi}_1^0}$ [5];

$$c\tau = \frac{1}{k_\gamma} \left(\frac{100 \text{ GeV}}{m_{\tilde{\chi}_1^0}} \right)^5 \left(\frac{\sqrt{F_0}}{100 \text{ TeV}} \right)^4 \times 10^{-2} \text{ cm} , \quad (11)$$

where $k_\gamma = |N_{11} \cos \theta_W + N_{12} \sin \theta_W|^2$ with θ_W being the Weinberg angle, and N_{ij} is the neutralino mixing angles. The constant is $k_\gamma = \cos^2 \theta_W$ for the bino-like $\tilde{\chi}_1^0$. The parameter F_0 is also related to the gravitino mass itself [3, 4];

$$m_{\tilde{G}} = \frac{1}{\sqrt{3}} \frac{F_0}{M_{pl}} = \left(\frac{\sqrt{F_0}}{100 \text{ TeV}} \right)^2 2.4 \text{ eV}. \quad (12)$$

The sensitivity to the neutralino lifetime is about 4% for $c\tau \sim 100$ cm as given in the previous section. Ignoring the errors of the neutralino mass and k_γ , this is translated to an error of about 1% for $\sqrt{F_0}$. The lifetime $c\tau = 100$ cm corresponds to $\sqrt{F_0} \sim 1000$ TeV and $m_{\tilde{G}} \sim 0.2$ keV, respectively.

If $c\tau$ is $\mathcal{O}(10) \sim \mathcal{O}(100)$ m, the ratio of the number of $\ell\gamma$ pairs to that of SUGRA-like events is a more sensitive measure for the lifetime. For $c\tau = 2000$ cm ($\sqrt{F_0} \sim 2400$ TeV and $m_{\tilde{G}} \sim 1.4$ keV), the estimated error is about 4%. This corresponds to a 1(2)% error

on $\sqrt{F_0}$ ($m_{\tilde{G}}$). The mass error of $\tilde{\chi}_1^0$ is estimated to be around 3%, because the number of events with a converted photon is around 100 for an integrated luminosity of 100 fb^{-1} , which is obtained in one year at the high luminosity runs of the LHC. From Eqs. (10) and (12) the error of F_0 ($m_{\tilde{G}}$) due to the mass error is 3(6)% in this case. For $c\tau = 10^4 \text{ cm}$ the number of events with a lepton and a converted photon is about 70 for the ultimate integrated luminosity of 300 fb^{-1} .

The above estimate is rather optimistic because we do not consider systematic errors of the measurement. In addition, we have so far not considered the effect of background events from the Standard Model processes and the SUSY production itself, where prompt photons from the interaction point mimic non-pointing photons due to the limited detector resolution. Note that in our Monte Carlo sample, 28757 sleptons are produced, and ~ 2500 (~ 70) of them are accepted as the sample with a (converted) non-pointing photon for $c\tau = 300 \text{ cm}$. Especially for a large $c\tau$ case, the number of real non-pointing photons is small and the analysis might severely suffer from the background. Studies with full detector simulations are necessary to understand the systematic errors and the background, and should be completed before the start of the LHC physics run. If events with a non-pointing photon converting in the TRT cannot be used for mass reconstruction due to the backgrounds, the $\Delta m_{\tilde{\chi}_1^0} \sim 30 \%$ is expected from the endpoint analysis involving jets and leptons. In this case the uncertainty of the neutralino mass would lead to an error of the gravitino mass by a factor of two.

Acknowledgments

We thank the ATLAS collaboration members for useful discussion. We have made use of the physics analysis framework and tools which are the result of collaboration-wide efforts. We especially thank Dr. J. Kanzaki and D. Toya. We also thank Dr. G. Polesello for useful suggestions. This work is supported in part by the Grant-in-Aid for Science Research, Ministry of Education, Science and Culture, Japan (No.11207101 and 15340076 for K.K., and No.14540260 and 14046210 for M.M.N.). M.M.N. is also supported in part by a Grant-

- [1] M. Dine, A. E. Nelson, Y. Nir, and Y. Shirman, *Phys. Rev. D* **53**, 2658 (1996).
- [2] G. F. Giudice and R. Rattazzi, *Phys. Rept.* **322**, 419 (1999).
- [3] D. V. Volkov and V. A. Soroka, *JETP Lett.* **18**, 312 (1973) [*Pisma Zh. Eksp. Teor. Fiz.* **18**, 529 (1973)].
- [4] S. Deser and B. Zumino, *Phys. Rev. Lett.* **38**, 1433 (1977).
- [5] P. Fayet, *Phys. Lett. B* **70**, 461 (1977); **84**, 416 (1979).
- [6] S. Ambrosanio *et al.*, *Phys. Rev. D* **54**, 5395 (1996).
- [7] S. Dimopoulos, S. Thomas, and J. D. Wells, *Nucl. Phys. B* **488**, 39 (1997).
- [8] J. A. Bagger, K. T. Matchev, D. M. Pierce, and R. J. Zhang, *Phys. Rev. D* **55**, 3188 (1997).
- [9] ATLAS: Detector and physics performance technical design report, CERN-LHCC-99-14.
- [10] I. Hinchliffe and F. E. Paige, *Phys. Rev. D* **60**, 095002 (1999).
- [11] S. P. Martin, *Phys. Rev. D* **55**, 3177 (1997).